Physica A 486 (2017) 674–680

Contents lists available at ScienceDirect

Physica A

journal homepage: www.elsevier.com/locate/physa

Route to chaos and some properties in the boundary crisis of a generalized logistic mapping

Diogo Ricardo da Costa [a,*], Rene O. Medrano-T [b], Edson Denis Leonel [a]

[a] Departamento de Física, UNESP — Univ. Estadual Paulista, Av.24A, 1515 - 13506-900 - Rio Claro - SP, Brazil
[b] Departamento de Ciências Exatas e da Terra, UNIFESP — Univ. Federal de São Paulo - Rua São Nicolau, 210, Centro, 09913-030, Diadema, SP, Brazil

HIGHLIGHTS

- A generalization of the logistic map is considered.
- A parametric perturbation is introduced in the system.
- Some results at the boundary crisis are obtained.

ARTICLE INFO

Article history:
Received 22 December 2016
Received in revised form 13 April 2017
Available online 3 June 2017

Keywords:
Boundary crisis
Feigenbaum universality
Generalized logistic mapping

ABSTRACT

A generalization of the logistic map is considered, showing two control parameters α and β that can reproduce different logistic mappings, including the traditional second degree logistic map, cubic, quartic and all other degrees. We introduce a parametric perturbation such that the original logistic map control parameter R changes its value periodically according an additional parameter $\omega = 2/q$. The value of q gives this period. For this system, an analytical expression is obtained for the first bifurcation that starts a period-doubling cascade and, using the Feigenbaum Universality, we found numerically the accumulation point R_c where the cascade finishes giving place to chaos. In the second part of the paper we study the death of this chaotic behavior due to a boundary crisis. At the boundary crisis, orbits can reach a maximum value $X = X_{\max} = 1$. When it occurs, the trajectory is mapped to a fixed point at $X = 0$. We show that there exist a general recursive formula for initial conditions that lead to $X = X_{\max}$.

1. Introduction

The one-dimensional logistic map has been widely studied along the years, and its importance arises because it describes the typical behavior of many dissipative dynamical systems modeled by nonlinear differential equations [1–5]. Applications involve different areas, including biology, mathematics, engineering, physics and many others [6–17]. It is known that the usual second polynomial degree logistic mapping has some special characteristics, for example, it presents cascades of period-doubling bifurcations leading to chaos [18], tangent bifurcations giving rise to periodic windows, intermittent behavior and crisis events (boundary, interior and merging chaotic bands crisis) [19,20]. The logistic map belongs to the class of unimodal mappings and it is a model to biological population dynamics [21,22].

* Corresponding author.
E-mail address: diogocost2@gmail.com (D.R. da Costa).

http://dx.doi.org/10.1016/j.physa.2017.05.074
0378-4371/

Other works can be cited as examples of applications of the Logistic-like map, for example, the B-Exponential map, which can be used to generate pseudo-random numbers [23] as well as the regular logistic map [24].

In this paper we consider a generalization of the logistic mapping,

$$X_{n+1} = R_n X_n^{\alpha}\left(1 - X_n^{\beta}\right), \tag{1}$$

where X is the dynamical variable of the system, and α and β are two control parameters that can be chosen to reproduce not just the traditional second degree logistic map [6,22,25], when R_n is constant and $\alpha = \beta = 1$, but the cubic [6,26], and quartic maps, as well. We aim to understand and describe analytically the first flip bifurcation when varying the control parameters. With this result it will be possible to obtain the accumulation point using Feigenbaum universality. In the other part of the paper we study what happens in the boundary crisis, where we will find some analytical expressions for the curves of maximum value of X as function of the control parameters. The analytical and numerical results will be shown to be in good agreement. In our study, we explore the case $\alpha = \beta$. Typically, as the control parameter R_n varies, attractors arise [2] or change stability. Thus, following Refs. [2,3], we consider that R_n has a parametric perturbation given by

$$R_n(\epsilon, \omega) = R\left[1 + \epsilon \cos(\omega n \pi)\right]. \tag{2}$$

Here R is a control parameter and ϵ gives us the amplitude of the parametric perturbation. We call as an initial condition the set X_0 and R_0. The parameter ω affects the periodicity of the perturbation. This parametric perturbation can be used to generate strange non-chaotic attractors, which were discussed by Grebogi et al. in Ref. [27]. In this paper we consider periodic perturbation, so it is interesting to express $\omega = 2/q$, with q a non-zero natural value: the argument of Eq. (2) becomes $n2\pi/q$ where q gives the period of R_n. For example, $\omega = 2$ $(q = 1)$ leads to

$$R_0 = R_1 = R_2 = \cdots = R_M = R(1 + \epsilon), \tag{3}$$

for any M. For $\omega = 1$ $(q = 2)$, R_n is a period 2 function since $R_2 = R_0$, where

$$\begin{aligned} R_0 &= R(1 + \epsilon), \\ R_1 &= R(1 - \epsilon), \\ R_2 &= R(1 + \epsilon). \end{aligned} \tag{4}$$

A period 3, $R_3 = R_0$, is obtained considering $\omega = 2/3$ $(q = 3)$ with

$$\begin{aligned} R_0 &= R\left(1 + \epsilon\right), \\ R_1 &= R\left(1 - \epsilon/2\right), \\ R_2 &= R\left(1 - \epsilon/2\right), \\ R_3 &= R\left(1 + \epsilon\right). \end{aligned} \tag{5}$$

The procedure can be followed for any period q. It is important to observe that R_0 is equal to $R(1 + \epsilon)$ for any integer ω.

In the first part of the paper (Section 2) we show an analytical expression for the first flip bifurcation of the generalized logistic map periodically perturbed Eq. (1), leading a way to obtain numerically the accumulation point using the Feigenbaum universality. Next, at Section 3 we show important results at the boundary crisis. When the boundary crisis happens an abrupt destruction of the chaotic attractor occurs, leading some orbits to reach $X = 1$ and then $X = 0$. A recursive formulae is obtained, which shows the initial conditions that lead to $X = 1$. When it happens all the next iterations are equal to zero. The conclusions are drawn in Section 4.

2. Bifurcation diagram and the Feigenbaum universality

Bifurcation diagrams for the generalized logistic map are shown in Fig. 1. A typical behavior is observed where the initial periodic dynamic is conduced to chaos via successive flip bifurcations at a certain critical parameter R_c. The period 1 bifurcates to period 2 in R_{F_1} which becomes to period 4 in R_{F_2} and so on, constituting the Feigenbaum route to chaos. The accumulation point R_c can be determined following the expression

$$R_c = \lim_{j\to\infty}\left(R_{F_{j+1}} + \frac{R_{F_{j+1}} - R_{F_j}}{\delta}\right), \tag{6}$$

where $\delta \cong 4.669201609$ is the Feigenbaum's constant [18].

From Eq. (6), it is possible to obtain a first approximation of R_c determining R_{F_1} and R_{F_2}. Both values can be verified directly by bifurcation diagrams, as in Fig. 1, but, for $\omega = 2$, R_{F_1} is found analytically for any values of the control parameters. Considering the period 1 condition, $X_1 = X_0 \equiv X_*$, Eq. (1) results in

$$R(1 + \epsilon)X_*^{\alpha-1}\left(1 - X_*^{\beta}\right) = 1. \tag{7}$$

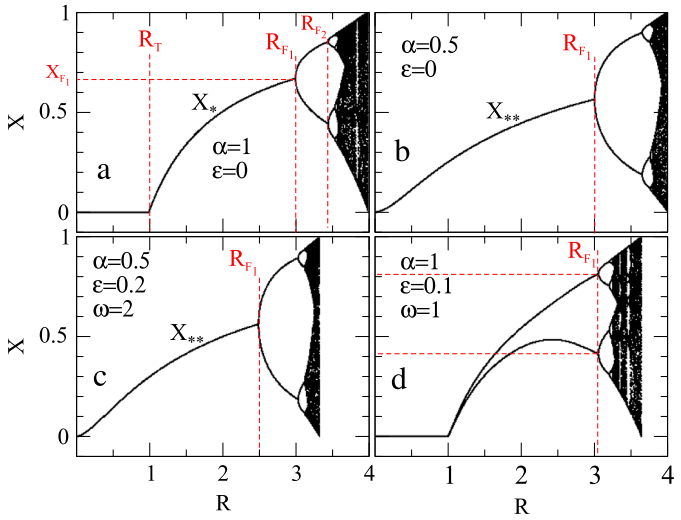

Fig. 1. Bifurcation diagrams for $\beta = \alpha$. (a) $\alpha = 1$ and $\epsilon = 0$, recovering the logistic map; (b) $\alpha = 0.5$ and $\epsilon = 0$; (c) $\alpha = 0.5$, $\epsilon = 0.2$ and $\omega = 2$ ($q = 1$); (d) $\alpha = 1$, $\epsilon = 0.1$ and $\omega = 1$ ($q = 2$). The initial condition chosen was $X_0 = 0.4$ and after a transient time of 10^4 iterations the data was plotted.

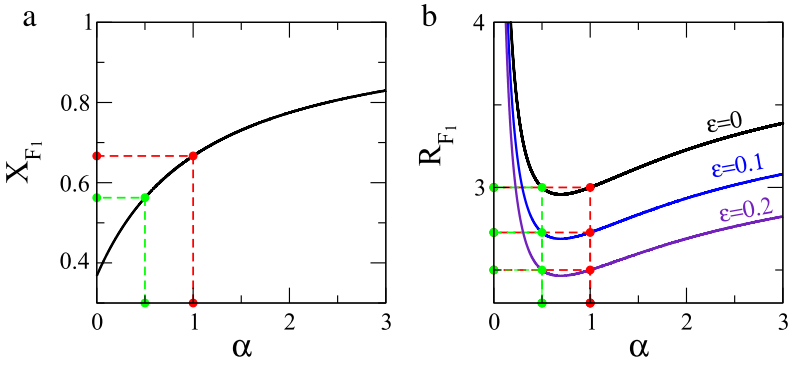

Fig. 2. (a) X_{F_1} vs α; (b) R_{F_1} vs α for $\omega = 2$ ($q = 1$) and $\beta = \alpha$.

A flip bifurcation occurs when $\frac{dX_{n+1}}{dX_n}|_{X_n=X_*} = -1$, given

$$R(1+\epsilon)X_*^{\alpha-1}\left[(\alpha+\beta)X_*^{\beta}-\alpha\right]=1. \tag{8}$$

Therefore, using Eqs. (7) and (8) we find the period 1 the first flip bifurcation which occurs at

$$X_{F_1}=\left(\frac{1+\alpha}{1+\alpha+\beta}\right)^{1/\beta}. \tag{9}$$

Additionally, Eq. (9) in Eq. (7) conduces to

$$R_{F_1}=\frac{X_{F_1}^{1-\alpha}}{\left(1-X_{F_1}^{\beta}\right)(1+\epsilon)}. \tag{10}$$

Here, $X_{F_1} \neq \{0, 1\}$ since for these values, R is not defined in Eq. (1). In Fig. 2(a) and (b) we show, respectively, the graphs of X_{F_1} and R_{F_1} for our case $\alpha = \beta$. With these figures, it is straightforward to find the values of X_{F_1} and R_{F_1} for each combination of α and ϵ shown in Fig. 1(a–c), where $\omega = 2$. R_{F_2} is always obtained numerically by the bifurcation diagram.

The bifurcation diagram in Fig. 1(a) shows the regular second degree logistic mapping for $R_n = R$. In the interval $R \in [0, 1]$ the fixed point $X_* = 0$ is stable. A transcritical bifurcation at $R = R_T = 1$ changes the stability and the other fixed point $X_* = 1 - 1/R$ becomes stable. This orbit suffers a duplication of period when it assumes the value $X_{F_1} = 2/3$ at the parameter $R_{F_1} = 3$, as highlighted in Fig. 2. After that, other duplications occur at $R_{F_2}, R_{F_3}, R_{F_4}, \ldots$ following the Feigenbaum universality until reaching the chaos at the accumulation point. Using a numerical method we have estimated that $R_{F_6} \cong 3.5696916$ and

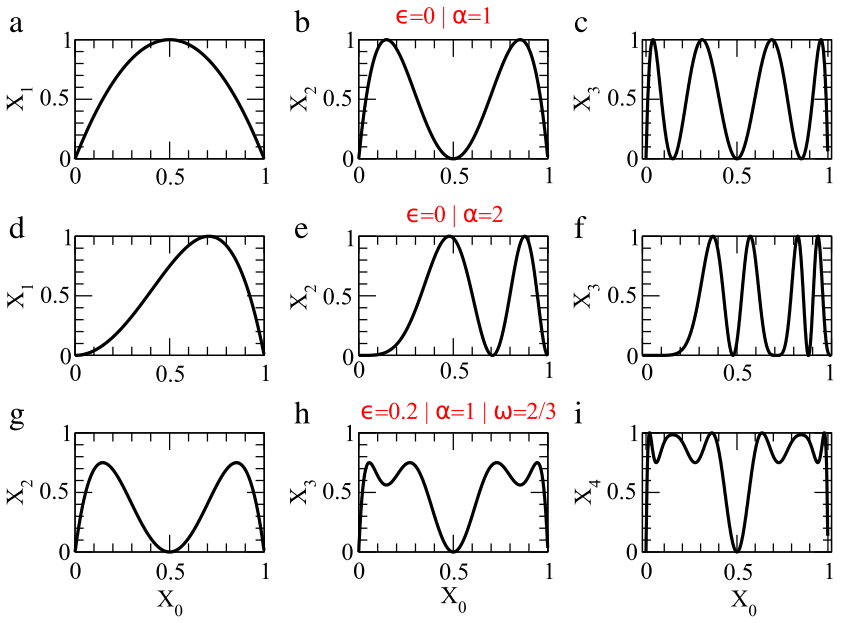

Fig. 3. For $R = 4/(1+\epsilon)$ and $\beta = \alpha$ we have in the items (a, b, c) the regular logistic map with $\epsilon = 0$ and $\alpha = 1$. The items (d, e, f) show X_1 vs X_0, X_2 vs X_0 and X_3 vs X_0 for $\epsilon = 0$ and $\alpha = 2$. For the items (g, h, i) we have the results considering $\alpha = 1$, $\omega = 2/3$ and $\epsilon = 0.2$.

$R_{F_7} \cong 3.5698913$. Therefore, the accumulation point obtained using Eq. (6) is $R_c \cong 3.56993$, which is in good agreement with the results found in Ref. [5].

For $\alpha = 0.5$ and $\epsilon = 0$ [Fig. 1(b)] no transcritical bifurcation occur. The expression of the fixed point in this interval is given by $X_{**} = \frac{1}{(1+1/R)^2}$. The first flip bifurcation still happens for $R_{F_1} = 3$ [see Fig. 2(b)]. We found by numerical method that $R_{F_6} \cong 3.7838474$ and $R_{F_7} \cong 3.7840656$, and using Eq. (6) we found $R_c \cong 3.78411$. In Fig. 1(c) a bifurcation diagram is shown for $\alpha = 0.5$ and $\epsilon = 0.2$, and one can see that $R_{F_1} = 2.5$ according to Fig. 2(b). Here the accumulation point found is $R_c \cong 3.15343$, where we found $R_{F_6} = 3.1532061$ and $R_{F_7} = 3.153388$. In the last picture Fig. 1(d), the parameters are $\alpha = 1$, $\epsilon = 0.1$ and $\omega = 1$. We can see that for $1 < R < 3$ the orbits have a period 2 due the value of $q = 2$ used in $\omega = 2/q$. For $R \gtrsim 3$ we have several duplications of period, determined just by numerical methods.

3. Boundary crisis

In the last section we presented a study about route to chaos in the generalized logistic map. Changing a parameter continuously, in general, chaos is suppressed by tangent bifurcation where a stable periodic orbit takes place restarting the route to chaos process again. Now we traverse the lost of the system stability where an abrupt destruction of the chaotic attractor occur. This phenomenon is due to a boundary crisis at $R_n = 4$, when the chaotic attractor touches an unstable period 1 orbit at $X = 0$ where the dynamics remains. For $R_n > 4$ the orbits no longer stay in the interval $X \in [0, 1]$. Observing Eq. (2) a maximum value of R_n, named as $(R_n)_{\max}$, is obtained when the cosine function is equal to $+1$. It happens for

$$(R_n)_{\max} = R(1+\epsilon). \tag{11}$$

If we consider $(R_n)_{\max} = 4$ then the boundary crisis value R_{BC} is

$$R_{BC} = \frac{4}{1+\epsilon}, \tag{12}$$

which is achieved just when the index n of the function R_n is a multiple of q, as shown in Eq. (11). If the index is not a multiple of q then $R_n < 4$. One can see that in Fig. 1(a) and (b), where $\epsilon = 0$, the boundary crisis occur at $R_{BC} = 4$ while, in Fig. 1(c) and (d), $R_{BC} < 4$ since $\epsilon > 0$. It is important to observe that R_{BC} in Eq. (12) is independent of the control parameter α.

At the boundary crisis, a special situation occurs. The dynamics is conduced to the unstable periodic orbit at $X = 0$ when it achieves $X = 1$. Therefore, for a better understanding about how the boundary crisis occur, it is interesting to find out which initial conditions lead the dynamics to $X = 1$ when $R = R_{BC}$. In Fig. 3(a), the first iteration of the mapping X_1 as function of the initial condition X_0 is shown for the logistic map. As one sees, $X_1 = 1$ is observed for the initial condition $X_0 = 1/2$. For two iterations of the mapping, the plot of X_2 as function of X_0 has as result Fig. 3(b). Now, for $X_0 = 1/2$ the value of X_2 is zero, and one can see that X_2 vs X_0 has two maximums ($M_2 = 2$) $X_2 = 1$. Increasing the number of iterations to

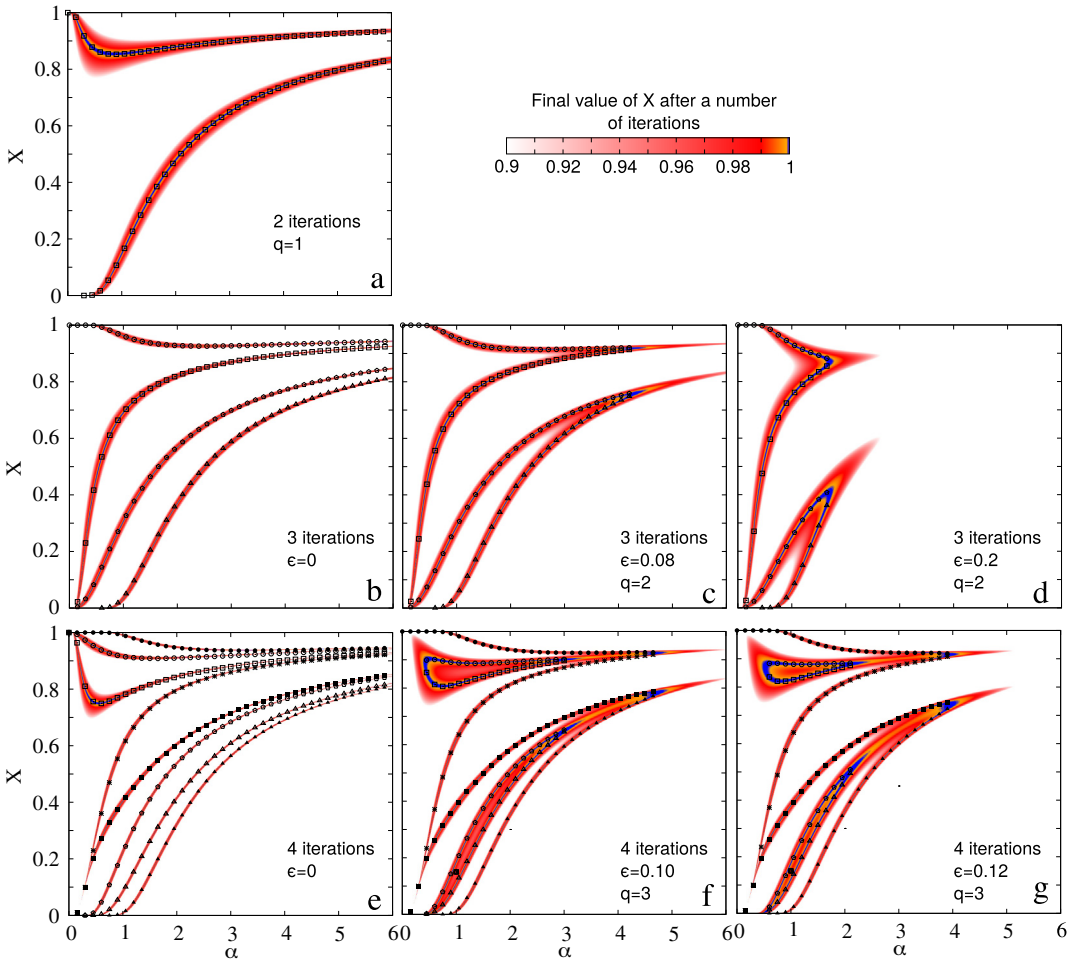

Fig. 4. In this figure we present X_0 as a function of α, where the color represents the value of the final X obtained after the iterations. We have considered in: (a) 2 iterations and $q = 1$; (b) 3 iterations and $\epsilon = 0$; (c) 3 iterations, $\epsilon = 0.08$ and $\omega = 2/2$; (d) 3 iterations, $\epsilon = 0.20$ and $\omega = 2/2$; (e) 4 iterations and $\epsilon = 0$; (f) 4 iterations, $\epsilon = 0.10$ and $\omega = 2/3$; (g) 4 iterations, $\epsilon = 0.12$ and $\omega = 2/3$; Rule for palette colors: $X < 0.9$ is represented by white, $X = 0.99$ corresponds to red, $X = 0.999$ to orange and $X = 1$ is colored in blue. The analytical results are represented as different symbols and $\beta = \alpha$. (For interpretation of the references to color in this figure legend, the reader is referred to the web version of this article.)

3 we obtain the plot shown in Fig. 3(c), and the number of maximums $X_3 = 1$ is equal to 4 ($M_3 = 4$). Therewith, the number of maximums $X_p = 1$ in the pth iteration is

$$M_p = 2^{p-1}. \tag{13}$$

Therefore, the probability of an orbit in the chaotic set touch the periodic orbit at a time p increases exponentially.

We start to change the other parameters. Initially the value of α is changed to $\alpha = 2$ and the position of the maximums are observed moving. For X_1 vs X_0, as shown in Fig. 3(d), the position of the maximum moves to approximately $X_0 = 0.7$. The graphics of X_2 vs X_0 and X_3 vs X_0 are shown in Fig. 3(e, f). As one can see the maximums are differently positioned when comparing to those in Fig. 3(b, c), but Eq. (13) still holds.

A more complicated behavior is observed when the parameter ω is changed with $\epsilon > 0$. In Fig. 3(g–i) we consider $q = 3$ and $\epsilon = 0.2$. For this case, R_1 and R_2, given by Eqs. (5), are less than 4 and the graph of the second (X_2) [Fig. 3(g)] and third (X_3) [Fig. 3(h)] iterations of the mapping are not higher than 0.8. In the other hand, the plot of the fourth iteration X_4 [Fig. 3(i)] has 6 local maximums $X_4 = 1$. For $\epsilon \neq 0$, Eq. (13) is not longer observed, and below we show a method to find the number of maximums.

A good way to visualize the maximums as function of the control parameters is to consider a plot as shown in Fig. 4. To construct these pictures we have made a grid of 1000 by 1000 equally spaced X_0 and α values. The final value of X after a number of iterations is determined by Eq. (1) for each (α, X_0) set with $\beta = \alpha$. If the final value of X is less then 0.9 we colored as white, while for $X \in [0.9, 1.0]$ the colors follow the palette in the Fig. 4. If $X \to 1$ then the color tends to blue, which represent the initial conditions that bring to a maximum X.

In Fig. 4(a) it is considered two iterations of the mapping for $\epsilon = 0$. As one sees, we have two curves that change as a function of α. Fig. 4(b) shows the results considering three iterations of the mapping and four different curves are observed with $\epsilon = 0$. In Fig. 4(e) the mapping was iterated up to four times for $\epsilon = 0$, and the number of maximums is 8. For $\alpha = 1$ these pictures express the results of the logistic map shown in Fig. 3(a–c). The number of maximums now is 8. It expresses that the exponential growth of M_n in Eq. (13) is independent of the parameters α when $\epsilon = 0$.

Now we take into account the parametric perturbations for different values of ϵ and $\omega = 2/q$. As mentioned before, for $\epsilon \neq 0, X = 1$ is only observed for $R_0 = R_q = R_{2q} = \cdots$. Thus, in Fig. 4(c) where $q = 2$ and $\epsilon = 0.08$ we consider three iterations of the mapping. As one sees, the four curves observed in Fig. 4(b) start connecting to each other. Increasing ϵ to 0.2 it generated Fig. 4(d), which shows that this curve is restricted to a limited interval of α. The same is observed for $q = 3$ when ϵ grows. Fig. 4(f) shows the results for $q = 3$ and $\epsilon = 0.10$. For 4 iterations, this mapping should present 8 maximums $X_4 = 1$ for each value of α as observed in the Fig. 4(e). Instead, there are four connections in Fig. 4(f), being two of them closed curves. Changing ϵ to 0.12 the connections are more clear (see Fig. 4(g)). In conclusion, the number of maximums $X = 1$ is highly affected by the value of the ϵ chosen. Therefore, with parametric perturbations ($\epsilon \neq 0$), the number of maximums observed does not follow that one observed for $\epsilon = 0$. Instead, Eq. (13) is the upper limit of this number.

Now we derive a general equation that describes how trajectories are conduced to the unstable periodic point $X = 0$. For convenience we denote the iteration and the parametric perturbation just before to the boundary crisis as $X_{q+1} = 1$ and $R_q = 4$, respectively. Therefore, here $R = 4/(1+\epsilon)$ and, following Eq. (1) with $\alpha = \beta$,

$$X_q = \left(\frac{1}{2}\right)^{\frac{1}{\alpha}}, \tag{14}$$

$$X_{q-1} = \left(\frac{1}{2} \pm \frac{1}{2}\sqrt{1 - 4\frac{X_q}{R_{q-1}}}\right)^{\frac{1}{\alpha}}, \tag{15}$$

$$X_{q-2} = \left(\frac{1}{2} \pm \frac{1}{2}\sqrt{1 - 4\frac{X_{q-1}}{R_{q-2}}}\right)^{\frac{1}{\alpha}}, \tag{16}$$

$$\vdots$$

$$X_1 = \left(\frac{1}{2} \pm \frac{1}{2}\sqrt{1 - 4\frac{X_2}{R_1}}\right)^{\frac{1}{\alpha}}, \tag{17}$$

$$X_0 = \left(\frac{1}{2} \pm \frac{1}{2}\sqrt{1 - 4\frac{X_1}{R_0}}\right)^{\frac{1}{\alpha}}, \tag{18}$$

where

$$R_m = \frac{4}{1+\epsilon}\left[1 + \epsilon\cos\left(2\pi\frac{m}{q}\right)\right], \quad m = 0, \ldots, q. \tag{19}$$

For example, for $q = 1$, the parametric perturbation has just one value, $R_1 = R_2 = \cdots = 4$, so following Eq. (18) we have

$$X_2 = 1, \tag{20}$$

$$X_1 = \left(\frac{1}{2}\right)^{\frac{1}{\alpha}}, \tag{21}$$

$$X_0 = \left(\frac{1}{2} \pm \frac{1}{2}\sqrt{1 - X_1}\right)^{\frac{1}{\alpha}}. \tag{22}$$

In this case, X_0 has two solutions due the plus and minus sign at the square root. These two solutions lead to $X = 1$ after 2 iterations. There are always two independent curves of X_n as shown in Fig. 4(a). The analytical results are highlighted by different symbols (squares, circles, triangles, etc.) in Fig. 4.

A more interesting case is $q = 2$ where the perturbation assumes two different values: $R_1 = 4\frac{1-\epsilon}{1+\epsilon}$ and $R_2 = 4$. Thus,

$$X_3 = 1, \tag{23}$$

$$X_2 = \left(\frac{1}{2}\right)^{\frac{1}{\alpha}}, \tag{24}$$

$$X_1 = \left(\frac{1}{2} \pm \frac{1}{2}\sqrt{1 - 4\frac{X_2}{R_1}}\right)^{\frac{1}{\alpha}}, \tag{25}$$

$$X_0 = \left(\frac{1}{2} \pm \frac{1}{2}\sqrt{1 - X_1}\right)^{\frac{1}{\alpha}}. \tag{26}$$

In this case, four different solutions of X_0 are obtained and the results are shown in Fig. 4(b), for $\epsilon = 0$. After increasing the value of ϵ, the curves start to connect each other, as observed in Fig. 4(c)–(d) for $\epsilon = 0.08$ and $\epsilon = 0.2$ respectively. This result is in agreement of our solution since R_1 must be greater than $4X_2$ in Eq. (25). Similarly, for $q = 3$, eight independent solutions of X_n can be found for $\epsilon = 0$, as shown in Fig. 4(e). When ϵ increases, the curves start to connect each other, as Fig. 4(f)–(g) show.

Just to emphasize the complexity of the solutions, let us for example consider the regular logistic map with $\alpha = 1$ and $\epsilon = 0$. In this case, an orbit iterated many times has as solution X the following expression:

$$X = \frac{1}{2}\left(1 \pm \sqrt{1 - \frac{1}{2}\left(1 \pm \sqrt{1 - \frac{1}{2}\left(1 \pm \sqrt{\ldots}\right)}\right)}\right). \tag{27}$$

Depending on the combination of signals considered (plus or minus), the number of solutions for the maximum X is too high.

4. Conclusions

A generalization of the logistic mapping was studied. The map has two control parameter α and β that change the characteristics of the map, and using this one can reproduce some results, for example, for the quartic, cubic and second degree logistic mappings. A parametric perturbation was also introduced in the system. In the first part of the paper the first flip bifurcation was obtained analytically. With this result, we obtained the accumulation point using the Feigenbaum universality. At the boundary crisis, we found analytical expressions for the curves of maximum value of X as function of the control parameters. The analytical results were compared with the numerical ones, which are in good agreement.

Acknowledgments

DRC acknowledges Brazilian agency FAPESP (2013/22764-2). EDL thanks to CNPq, FUNDUNESP and FAPESP (2012/23688-5, 2008/57528-9 e 2005/56253-8), Brazilian agencies. This research was supported by resources supplied by the Center for Scientific Computing (NCC/GridUNESP) of the São Paulo State University (UNESP).

References

[1] D.R. da Costa, et al., Phys. Lett. A 380 (2016) 1610–1614.
[2] E.D. Leonel, J.K.L. da Silva, S.O. Kamphorst, Int. J Bifurc. Chaos 12 (2002) 1667–1674.
[3] E.D. Leonel, J.K.L. da Silva, S.O. Kamphorst, Physica A 295 (2001) 280–284.
[4] A.J. Lichtenberg, M.A. Lieberman, Regular and Chaotic Dynamics, in: Applied Mathematical Sciences, vol. 38, Springer-Verlag, New York, 1992.
[5] K.T. Alligood, T.D. Sauer, J.A. Yorke, Chaos: An Introduction to Dynamical Systems, Springer-Verlag, New York, 1996.
[6] J.A. de Oliveira, E.R. Papesso, E.D. Leonel, Entropy 15 (2013) 4310–4318.
[7] P.M. Gade, G.G. Sahasrabudhe, Phys. Rev. E 87 (2013) 052905.
[8] J.D. Challenger, D. Fanelli, A.J. McKane, Phys. Rev. E 88 (2013) 040102(R).
[9] R.T. Cerbus, W.I. Goldburg, Phys. Rev. E 88 (2013) 053012.
[10] K. Hamacher, Chaos 22 (2012) 033149.
[11] M. McCartney, Chaos 21 (2012) 043104.
[12] P. Philominathan, et al., Int. J. Bifurc. Chaos 21 (2011) 1927–1933.
[13] W. Hu, et al., Acta Phys. Sin. 17 (2012) 170505.
[14] M. Urquizu, A.M. Correig, Chaos Solitons Fractals 33 (2007) 1292–1306.
[15] D. Ilhem, K. Amel, Discret. Dyn. Nat. Soc. 2006 (2006) 15840.
[16] T.Y. Li, J.A. Yorke, Am. Math. Mon. 82 (1975) 985–992.
[17] R.M. May, G.A. Oster, Am. Nat. 110 (1976) 573–599.
[18] M.J. Feigenbaum, J. Stat. Phys. 19 (1) (1978) 25–52.
[19] C. Grebogi, E. Ott, J.A. Yorke, Phys. Rev. Lett. 48 (1982) 1507–1510.
[20] C. Grebogi, E. Ott, J.A. Yorke, Physica D7 (1983) 181–200.
[21] R. May, Nature 261 (1976) 459–467.
[22] Morris W. Hirsch, Stephen Smale, Robert L. Devaney, Differential Equations, Dynamical Systems, and an Introduction to Chaos, Ed. Elsevier Academic Press, 2004.
[23] M.C. Shastry, N. Nagaraj, P.G Vaidya, 2006, arXiv:cs/0607069 [cs.CR].
[24] K.J. Persohn, R.J. Povinelli, Chaos Solitons Fractals 45 (2012) 238–245.
[25] A.G. Radwan, J. Adv. Res. 4 (2013) 163–171.
[26] W.F. Ames, C. Rogers, Nonlinear Equations in the Applied Sciences, Ed. Academic Press, Inc., 1992.
[27] C. Grebogi, E. Ott, S. Pelikan, J.A. Yorke, Physica D 13 (1–2) (1984) 261–268.